Available online at www.derpharmachemica.com

Scholars Research Library

Der Pharma Chemica, 2015, 7(8):252-264
(http://derpharmachemica.com/archive.html)

ISSN 0975-413X
CODEN (USA): PCHHAX

Chemical constituents and corrosion inhibition of mild steel by the essential oil of *Thymus algeriensis* in 1.0 M hydrochloric acid solution

I. Hamdani[1], E. El Ouariachi[1], O. Mokhtari[2], A. Salhi[1], N. Chahboun[3,4], B. ElMahi[1], A. Bouyanzer[1], A. Zarrouk[1], B. Hammouti[1] and J. Costa[5]

[1]*LCAE-URAC 18, Faculty of Science, First Mohammed University, Oujda, Morocco*
[2]*Laboratoire de Géo-ressources et Environnement, Faculté des Sciences et Techniques, Université Sidi Mohammed Ben Abdallah, Fès, Morocco*
[3]*Laboratoire de Biotechnologie, Environnement et Qualité (LABEQ), Département de Biologie, Faculté des Sciences, Université Ibn Tofaïl, Kenitra, Morocco*
[4]*Laboratoire de procédés de séparation, Département de chimie, Faculté des Sciences, université Ibn Tofail, Kenitra, Morocco*
[5]*Laboratoire de Chimie des Produits Naturels, Faculté des Sciences et Techniques, Université de Corse, Corse, France*

ABSTRACT

Essential oil of aerial parts of Thymus algeriensis was obtained by hydrodistillation and analyzed by GC and GC/MS. 44 components were identified accounting 90.2% of the total oil, which borneol (28%), camphene (20.9%) and camphre (15.7%) were the major compounds. Inhibition effect of this essential oil (EOTA) on mild mild steel in 1.0 M HCl solution was studied. Inhibition efficiency of plant extracts were carried out by using chemical (weight loss method) and electrochemical techniques (potentiodynamic polarization and electrochemical impedance spectroscopy). The effect of temperature on the corrosion behavior of mild steel in 1.0 M HCl with addition of plant extracts was studied in the temperature range of 308 - 343 K. The adsorption and kinetic parameters for mild steel/EOTA/1.0 M HCl system were calculated from experimental gravimetric data and the interpretation of the results are given. The polarization studies showed that J EOTA acts as mixed-type inhibitor. The Nyquist plots showed that on increasing EOTA concentration, increases charge transfer resistance and decreases double layer capacitance. EOTA obeys the Langmuir adsorption isotherm.

Keywords: *Thymus algeriensis*, Hydrodistillation, Essential oil, Corrosion inhibition, Mild steel, Acid.

INTRODUCTION

Use of inhibitors is one of the most practical methods for protection against corrosion especially in acid solutions to prevent unexpected metal dissolution and acid consumption [1]. Different organic and non-organic compounds have been studied as inhibitors to protect metals from corrosion attack. Usually, organic compounds that exert a significant influence on the extent of adsorption on the metal surface and therefore can be used as effective corrosion inhibitors. The efficiency of these organic corrosion inhibitors is related to the presence of polar functions with S, O or N atoms in the molecule, heterocyclic compounds and π electrons [2-25]. The polar function is usually regarded as the reaction center for the establishment of the adsorption process [26].

Several studies indicated that most syntheses organic and inorganic inhibitors are toxic cause severe hazards to both human beings and environment during its applications [27,28]. Thus many researchers focus their efforts to replace these toxic inhibitors with nontoxic one, so there is a great interest toward the using of green corrosion inhibitors to

protect concrete rebar from corrosion because these inhibitors are not only nontoxic and environmental friendly, but also readily available and renewable [29-31].

Green inhibitors are reported to be low cost, safe, easily applicable, ecofriendly, preserve the environment and are easily available, they can be extracted by simple procedures with low cost from natural products such as plant extracts [32]. In addition, several works have been made to study the inhibition by essential oils on the corrosion of steel in acidic media and have been found to be very efficient corrosion inhibitors for mild steel in these acid media [33-36].

The *Thymus algeriensis* (Fig. 1), is a shrub up under more than 25 cm longth, a strong odor, pleasant flavoring, its flowering period lasts from April until July. In the present work, the chemical composition of *Thymus algeriensis* essential oil (EOTA) is established using GC and GC-MS. Then, the inhibition performance of EOTA was evaluated by weight loss measurement and electrochemical techniques. The thermodynamic parameters for both adsorption and activation processes were calculated and discussed.

Figure 1. *Thymus algeriensis*, in Oujda Eastern Morocco

MATERIALS AND METHODS

Inhibitor

Plant material

The aerial part of *Thymus algeriensis* was harvested in May 2015 of the Forest Sidi Maafa, in Oujda Eastern Morocco. A voucher specimen was deposited in the Herbarium of Faculty of Sciences, Oujda, Morocco. The dried plant material is stored in the laboratory at room temperature (298 K) and in the shade before the extraction

Hydrodistillation apparatus and procedure

Hydrodistillation is an extraction method whose function is to extract the volatile compounds of natural products with water vapour, and is often performed using Clevenger-type apparatus (Fig. 1), with 400 mL for 3 h. The essential oil yields were measured and subsequently dried over anhydrous sodium sulfate and stored at 277K in the dark before gas chromatographic determination of its composition [37].

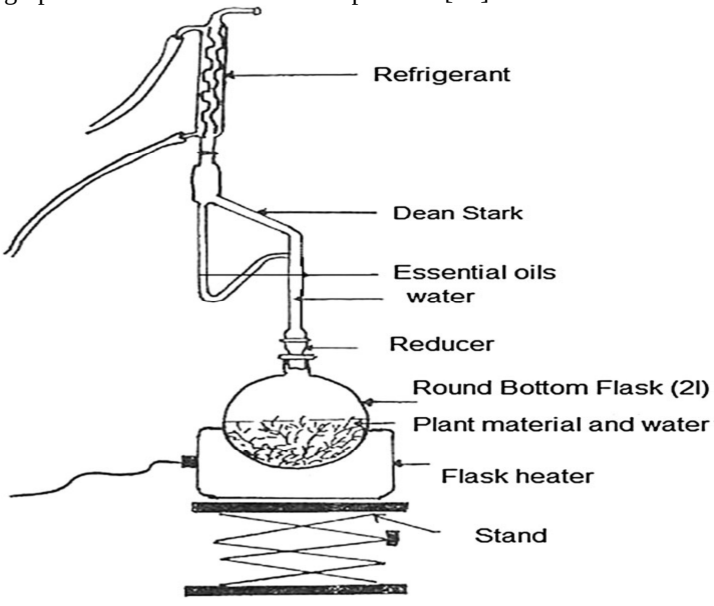

Figure 2: Hydrodistillation of essential oils: Clevenger-type apparatus

Characterization and chemical composition of essential oils

Techniques in chromatography (GC/MS, GC-FTIR, HPLC-DAD) are available for the molecular analysis of organic compounds. The chemical components of *Thymus algeriensis* essential oil was determined by spectral analysis of gas chromatography and gas chromatography coupled to mass spectrometry (GC-MS), which identified six major components. GC analyses were performed using a Perkin-Elmer Autosystem GC apparatus (Waltham, MA, USA) equipped with a single injector and two flame ionization detectors (FID). The apparatus was used for simultaneous sampling with two fused-silica capillary columns (60 m long with i.d. 0.22 mm, film thickness 0.25 µm) with different stationary phases: Rtx-1 (polydimethylsiloxane) and Rtx-Wax (polyethylene glycol). The temperature program was for 333-503K at 275K/min and then held at isothermal 503K (30 min). The carrier gas was helium (1 mL/min). Injector and detector temperatures were held at 553K. Split injection was conducted with a ratio split of 1:80. Electron ionization mass spectra were acquired with a mass range of 35-350 Da. The injected volume of oil was 0.1 µL. For gas chromatography–mass spectrometry, the oils obtained were investigated using a Perkin-Elmer Turbo Mass Quadrupole Detector, directly coupled to a Perkin-Elmer Auto system XL equipped with two fused-silica capillary columns (60 m long with i.d. 0.22 mm, film thickness 0.25 µm), with Rtx-1 (polydimethylsiloxane) and Rtx-Wax (polyethylene glycol). Other GC conditions were the same as described above. Ion source temperature was 423 K and energy ionization 70 eV. Electron ionization mass spectra were acquired with a mass range of 35-350 Da.

The injected volume of oil was 0.1 µL. Identification of the components was based (1) on the comparison of their GC retention indices (RI) on non-polar and polar columns, determined relative to the retention time of a series of n-alkanes with linear interpolation, with those of authentic compounds or literature data [33], and (2) on computer matching with commercial mass spectral libraries [33,34] and comparison of spectra with those in our personal library. Relative amounts of individual components were calculated on the basis of their GC peak areas on the two capillary Rtx-1 and Rtx-Wax columns, without FID response factor correction.

Materials

The steel used in this study is a carbon steel with a chemical composition 0.09 wt. % P; 0.38 wt. % Si; 0.01 wt. % Al; 0.05 wt. % Mn; 0.21 wt. % C; 0.05 wt. % S and the remainder iron (Fe).

Preparation of solutions

The aggressive solutions of 1.0 M HCl were prepared by dilution of analytical grade 37% HCl with distilled water. Inhibitor were dissolved in acid solution at the required concentrations (in g/L), and the solution in the absence of inhibitor was taken as blank for comparison purposes. The test solutions were freshly prepared before each experiment by adding essential oil of *Thymus algeriensis* directly to the corrosive solution. Concentrations of essential oils are 0.125, 0.25, 0.5 and 1g/L.

Gravimetric study

Gravimetric experiments were performed according to the standard methods [38], the mild steel sheets of 1 × 1 × 0.1 cm were abraded with a series of emery papers SiC (120, 600 and 1200) and then washed with distilled water and acetone. After weighing accurately, the specimens were immersed in a 100 mL beaker containing 250 mL of 1.0 M HCl solution with and without addition of different concentrations inhibitor. All the aggressive acid solutions were open to air. After 6 h of acid immersion, the specimens were taken out, washed, dried, and weighed accurately. In order to get good reproducibility, all measurements were performed few times and average values were reported to obtain good reproducibility.

Electrochemical measurements

The electrochemical measurements were carried out using Volta lab (Tacussel- Radiometer PGZ 100) potentiostate and controlled by Tacussel corrosion analysis software model (Voltamaster 4) at under static condition. The corrosion cell used had three electrodes. The reference electrode was a saturated calomel electrode (SCE). A platinum electrode was used as auxiliary electrode of surface area of 1 cm^2. The working electrode was mild steel of the surface 0.32 cm^2. All potentials given in this study were referred to this reference electrode. The working electrode was immersed in test solution for 30 min to a establish steady state open circuit potential (E_{ocp}). After measuring the E_{ocp}, the electrochemical measurements were performed. All electrochemical tests have been performed in aerated solutions at 308 K. The EIS experiments were conducted in the frequency range with high limit of 100 kHz and different low limit 0.1 Hz at open circuit potential, with 10 points per decade, at the rest potential, after 30 min of acid immersion, by applying 10 mV ac voltage peak-to-peak. Nyquist plots were made from these experiments. The best semicircle can be fit through the data points in the Nyquist plot using a non-linear least square fit so as to give the intersections with the *x*-axis.

The inhibition efficiency of the inhibitor was calculated from the charge transfer resistance values using the following equation:

$$\eta_z\% = \frac{R_{ct}^{i} - R_{ct}^{\circ}}{R_{ct}^{i}} \times 100 \quad (1)$$

Where, R°_{ct} and R^{i}_{ct} are the charge transfer resistance in absence and in presence of inhibitor, respectively.

After ac impedance test, the potentiodynamic polarization measurements of mild steel substrate in inhibited and uninhibited solution were scanned from cathodic to the anodic direction, with a scan rate of 1 mV s^{-1}. The potentiodynamic data were analysed using the polarization VoltaMaster 4 software. The linear Tafel segments of anodic and cathodic curves were extrapolated to corrosion potential to obtain corrosion current densities (I_{corr}). From the polarization curves obtained, the corrosion current (I_{corr}) was calculated by curve fitting using the equation:

$$I = I_{corr}\left[exp\left(\frac{2.3\Delta E}{\beta_a}\right) - exp\left(\frac{2.3\Delta E}{\beta_c}\right)\right] \quad (2)$$

The inhibition efficiency was evaluated from the measured I_{corr} values using the following relationship:

$$\eta_{Tafel}(\%) = \frac{I_{corr} - I_{corr(i)}}{I_{corr}} \times 100 \quad (3)$$

where I_{corr} and $I_{corr(i)}$ are the corrosion current densities for steel electrode in the uninhibited and inhibited solutions, respectively.

RESULTS AND DISCUSSION

Quantification of essential oil constituents

The analysis of essential oil from *Thymus algeriensis* was carried out by GC and GC/MS. The chemical composition of essential oil was characterized by 44 compounds, which accounted for 90.2% of the total oil. The retention time of volatile compounds (RIa and RIp) and their percentage are summarized in Table 1.

Table 1: Chemical composition of *Thymus algeriensis* essential oil from Morocco

Compounds	Ir *l*	Ir *a*	Ir *p*	%
α-Thujene	932	921	1020	0.4
α-Pinene	936	929	1020	7.2
Camphene	950	943	1065	12.1
Oct-1-en-3-ol	962	959	1438	0.2
Sabinene	973	964	1117	0.8
β-pinene	978	969	1107	3.5
Myrcene	987	980	1156	1.6
α-terpinene	1013	1008	1174	0.1
p-Cymene	1015	1011	1263	1.6
Cineole 1,8	1024	1020	1207	5.2
Limonene	1025	1020	1196	2.8
(Z)b-Ocimene	1029	1024	1226	0.1
(E)b-Ocimene	1041	1035	1243	1.1
g-terpinene	1051	1047	1239	0.3
E-hydrate de sabinene	1053	1052	1453	0.5
Z-hydrate de sabinene	1082	1080	1540	0.1
Linalol	1086	1083	1535	1.4
Camphre	1123	1123	1505	10.9
Trans pinocarveol	1126	1123	1666	1.0
Cis Verbenol	1132	1129	1657	0.3
Trans Verbenol	1136	1129	1666	0.6
Borneol	1150	1154	1691	28
Terpinen-4-ol	1164	1166	1589	1.6
a-Terpineol	1176	1175	1680	1.0
Verbenone	1183	1181	1715	0.2
Carvone	1214	1215	1722	0.2
Carvacrol methyl ether	1226	1225	1612	0.1
Geraniol	1235	1235	1829	0.2

Bornyl acetate	1270	1269	1570	1.0
Carvacrol	1278	1279	2190	0.3
Geranyl acetate	1362	1361	1745	1.4
α-copaene	1379	1374	1488	0.3
β-Bourbonene	1386	1382	1513	0.2
α-Gurjunene	1413	1408	1524	0.2
E-Caryophyllene	1421	1416	1593	0.5
Germacrene D	1479	1474	1699	0.7
Bicyclogermacrene	1494	1490	1722	0.1
β-Bisabolene	1503	1500	1718	0.8
δ-Cadinene	1520	1514	1763	0.3
Spathulenol	1572	1563	2101	0.5
Caryophyllene oxyde	1578	1568	1963	0.4
Viridiflorol	1592	1588	2083	0.1
α-cadinol	1643	1638	2209	0.3
α-bisabolol	1673	1666	2205	0.2
α-Thujene	932	921	1020	0.4
α-Pinene	936	929	1020	7.2
Camphene	950	943	1065	12.1
Oct-1-en-3-ol	962	959	1438	0.2
Sabinene	973	964	1117	0.8
β-pinene	978	969	1107	3.5
Myrcene	987	980	1156	1.6
α-terpinene	1013	1008	1174	0.1
p-Cymene	1015	1011	1263	1.6
Cineole 1,8	1024	1020	1207	5.2
Limonene	1025	1020	1196	2.8
Total				**90.2**

The most abundant compounds were borneol (28%), camphene (20.9%) and camphre (15.7%). These three compounds represent 64.6% of the total oils (Fig. 2).

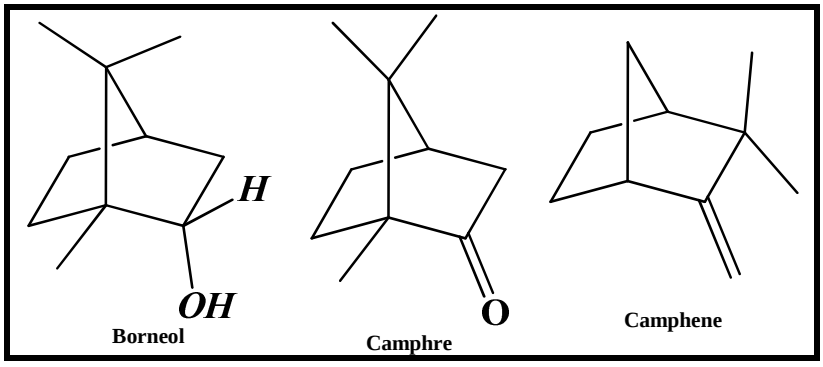

Figure 2: Chemical molecular structure of three major constituents of *Thymus algeriensis* essential oils

Corrosion inhibition evaluation

Effect of concentration inhibitor

Gravimetric measurements

The effect of addition of EOTA tested at different concentrations on the corrosion of mild steel in 1.0 M HCl solution was studied by weight loss method at 308 K after 6 h of immersion period. The corrosion rate (C_R) and inhibition efficiency $\eta_{WL}(\%)$ were calculated according to the Eqs. 4 and 5 [39,40], respectively:

$$C_R = \frac{W_b - W_a}{At} \quad (4)$$

$$\eta_{WL}(\%) = \left(1 - \frac{w_i}{w_0}\right) \times 100 \quad (5)$$

where W_b and W_a are the specimen weight before and after immersion in the tested solution, w_0 and w_i are the values of corrosion weight losses of mild steel in uninhibited and inhibited solutions, respectively, A the total area of the mild steel specimen (cm^2) and t is the exposure time (h).

The obtained values of corrosion rate (C_R) and inhibition efficiency η_{WL}(%) are summarized in Table 2. It is obvious from these results that the EOTA inhibits the corrosion of mild steel at all concentrations used in this study. The variation of C_R and η_{WL}(%) with the EOTA concentration are shown in Fig. 3. It can be observed from this figure, that the C_R of mild steel decreases while the protection efficiency increases as the EOTA concentration increases in 1.0 M HCl solutions. This conclusion was also supported by the electrochemical studies reported below. The maximum η_{WL} (%) of 81 % is achieved at 1g/L and a further increase in concentration did not cause any appreciable change in the performance of the inhibitor. Accordingly, the effectiveness of inhibiting corrosion by an essential oil is closely related to its chemical composition which includes a non-polar, hydrophobic, consisting of hydrocarbon molecules and a polar, hydrophilic, which presents one or more functional groups. Indeed, the inhibitive action of *Thymus algeriensis* essential oil could be attributed to the adsorption of its components on the mild steel surface by a synergistic action of oxygenated and hydrocarbon terpenes, especially their major constituents (Fig. 2).

Table 2: Gravimetric results of steel HCl at various concentrations of oil and extract of *Thymus algeriensis* at 308 K

Medium	Inhibitor (g/L)	C_R (mg cm^{-2} h^{-1})	η_{WL} (%)	θ
Blank	——	0.430	—	——
EOTA	0.125	0.192	55	0.55
	0.25	0.119	72	0.72
	0.5	0.100	76	0.76
	1.0	0.079	81	0.81

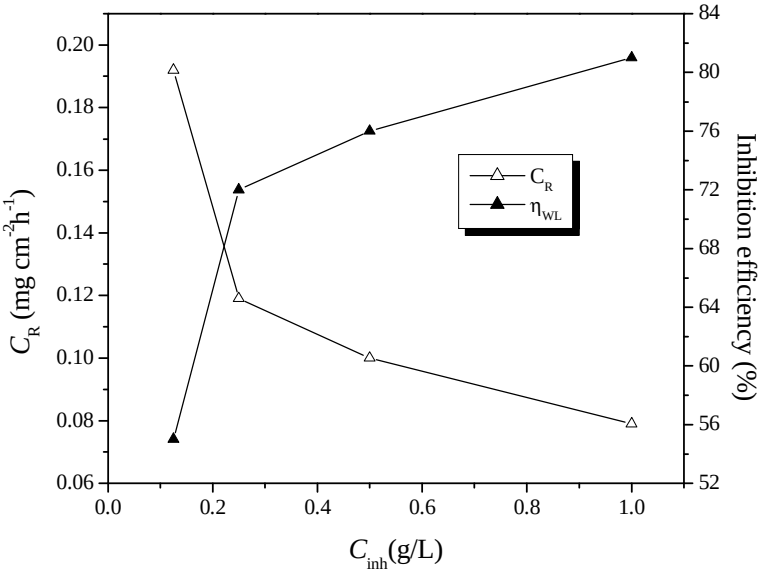

Figure 3. Variation of corrosion rate and inhibition efficiency of mild steel in 1.0 M HCl containing various concentrations of EOTA

Polarization measurements

Figure 4 shows the Tafel curves in 1.0 M HCl solutions with and without addition of EOTA at different concentrations. The corrosion current density decreases with increasing inhibitor concentrations and the corrosion potential shifts depending on the inhibitor concentration. The values of the electrochemical parameters obtained from the Tafel curves, namely: corrosion potential (E_{corr}), cathodic Tafel slope (β_c), anodic Tafel slope (β_a), corrosion current density (I_{corr}), inhibition efficiency η_{Tafel} (%) for the different concentrations of EOTA are given in Table 2.

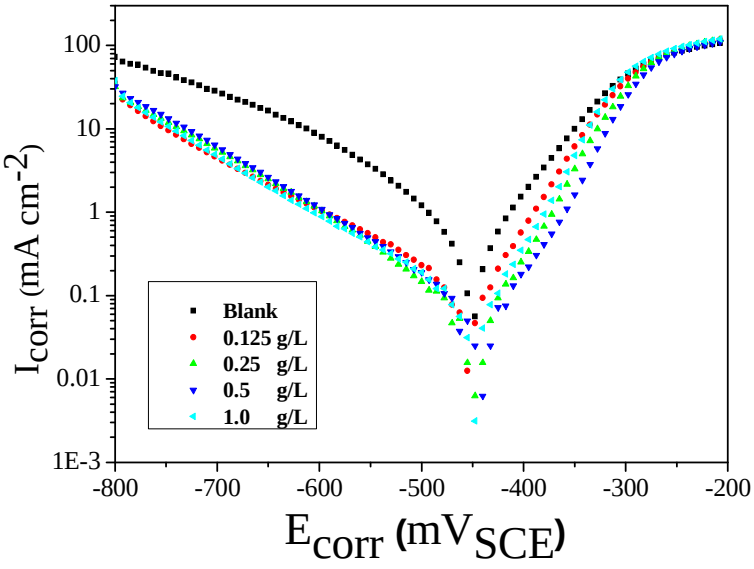

Figure 4: Tafel plot of mild steel with different concentrations of EOTA in 1.0 M HCl solution

Table 2. Tafel polarization parameters obtained at different concentrations of EOTA

Inhibitor	Conc (g/L)	$-E_{corr}$ (mV_{SCE})	β_a (mV/dec)	$-\beta_c$ (mV/dec)	I_{corr} ($\mu A\ cm^{-2}$)	η_{Tafel} (%)
1.0 M HCl	——	450	71.9	105.2	420.0	—
EOTA	0.125	453	61.1	165.4	135.5	67
	0.250	451	59.5	138.5	89.7	78
	0.500	447	57.7	137.8	80.6	94
	1.000	447	51.1	141.8	74.2	96

It can be seen from the Fig. 4 that, in the presence of inhibitor, the curves are shifted to lower current regions, showing the inhibition tendency of the EOTA. There was no definite trend is observed in the E_{corr} values in the presence of EOTA. In the present study, shift in E_{corr} values is in the range of 2-6 mV suggested that they all are acted as mixed type of inhibitor [41, 42]. Investigation of Table 2 revealed that the values of β_a change slightly in the presence of EOTA where as more pronounced change occurs in the values of β_c, indicating that both anodic and cathodic reactions are effected but the effect on the cathodic reactions is more prominent. Thus, EOTA acted as mixed type, but predominantly cathodic inhibitor [43].

Electrochemical impedance spectroscopy

The corrosion behaviour of mild steel in 1.0 M HCl solution in the presence of EOTA was investigated by EIS at 308 K after 30 min of immersion. Fig. 5 shows the results of EIS experiments in the Nyquist representation. After analyzing the shape of the Nyquist plots, it is concluded that the curves approximated by a single capacitive semi-circles, showing that the corrosion process was mainly charge transfer controlled [44]. The general shape of the curves is very similar for all samples; the shape is maintained throughout the whole concentrations, indicating that almost no change in the corrosion mechanism occurred due to the inhibitor addition [45]. The diameter of Nyquist plots (R_{ct}) increases on increasing the EOTA concentration. These results suggest the inhibition behaviour of EOTA on corrosion of mild steel in 1.0 M HCl solution.

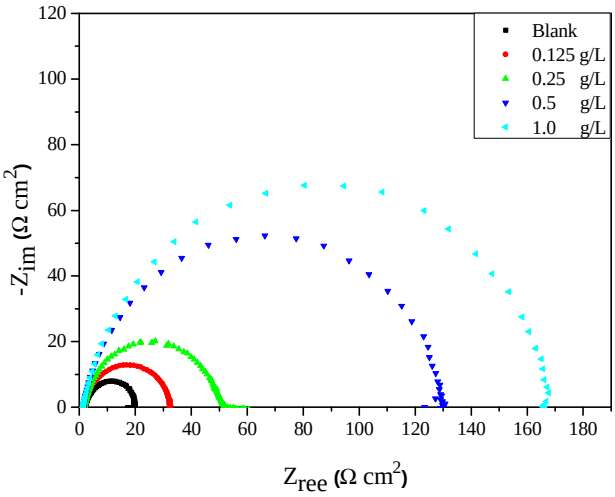

Figure 5: Nyquist plots for mild steel in 1.0 M HCl at 308 K containing different concentrations of EOTA

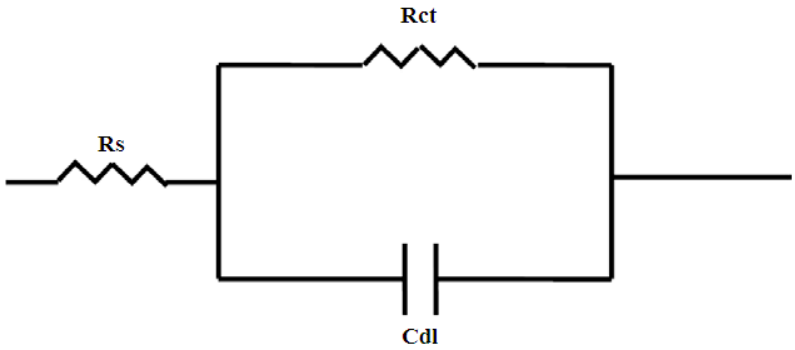

Figure 6: The equivalent circuit model

The Nyquist plots are analyzed in terms of the equivalent circuit composed with classic parallel capacitor and resistor (shown in Fig. 6) [46]. The impedance parameters including charge-transfer resistance R_{ct}, double layer capacitance C_{dl} and inhibition efficiency η_z% are given in Table 3. Charge-transfer resistance increases from 16.0 to 166.7 Ω cm^2 and double layer capacitance C_{dl} decreases from 84.0 to 60.4 µF/cm^2 with the increase of EOTA concentration. The decrease in C_{dl} means that the adsorption of inhibitor takes place on the mild steel surface in acidic solution. The increase in the charge-transfer resistance leads to an increase of inhibition efficiency. The results indicate good agreement between the values of corrosion efficiency as obtained from the weight loss, polarization measurements and impedance technique. It is concluded that the corrosion rate depends on the chemical nature of the electrolyte rather than the applied technique [46].

The double-layer capacitance (C_{dl}) was calculated from the following equation:

$$C_{dl} = \frac{1}{2\pi f_{max} R_{ct}} \qquad (6)$$

where f_{max} is the frequency at which the imaginary component of the impedance is maximal.

Table 3. Impedance parameters and inhibition efficiency for mild steel in 1.0 M HCl solutions containing different concentrations of EOTA

Conc (g/L)	R_s (Ω cm^2)	R_{ct} (Ω cm^2)	f_{max} (Hz)	C_{dl} (µF cm^{-2})	η_z (%)
1.0 M HCl	2.1	13.1	111.61	84.0	—
1.000	1.6	166.7	15.83	60.4	46
0.500	1.5	128.8	20.00	61.8	67
0.250	1.6	51.5	44.64	70.9	93
0.125	1.4	31.5	67.38	75.0	91

Adsorption isotherm behaviour

Basic information on the interaction between the organic inhibitor and the mild steel surface are obtained from various adsorption isotherms. The most commonly used adsorption isotherms are Langmuir, Temkin, and Frumkin isotherm. The degree of surface coverage (θ) for different concentrations of the inhibition in acidic media have been evaluated from weight loss measurements using the equation $\theta = (\eta_{WL}/100)$.The surface coverage values (θ) were tested graphically for fitting a suitable adsorption Isotherm. Plotting C_{inh}/θ vs. C_{inh} yielded a straight line [Fig. 7] with correlation coefficient (R^2) value given in Table 4 at 308 K. The R^2 value (0.99912) is near to unity indicating that the adsorption of this inhibitor obey the Langmuir adsorption isotherm represented by the following equation.

$$\frac{C_{inh}}{\theta} = \frac{1}{K_{ads}} + C_{inh} \qquad (7)$$

where C_{inh} is the equilibrium inhibitor concentration, K_{ads} adsorptive equilibrium constant.

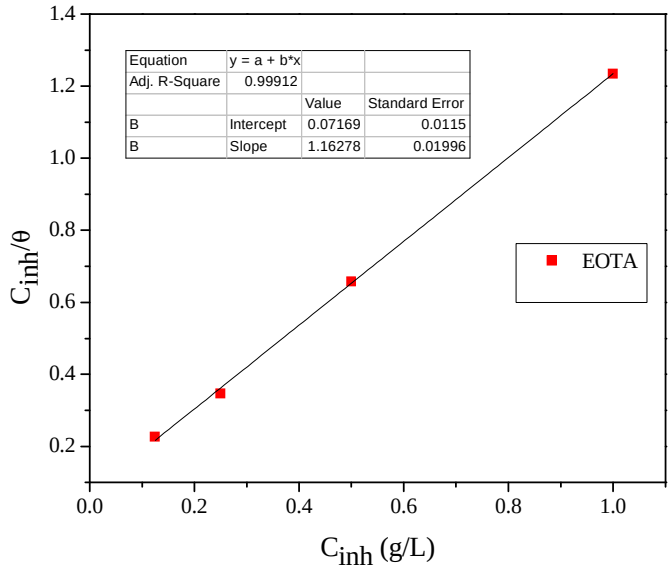

Figure 7: Langmuir adsorption isotherm for mild carbon steel in 0.1 M HCl solutions containing *Thymus algeriensis* essential oil

On the other hand, this isotherm postulates that there is no interaction between the adsorbed molecules. The calculation of the standard free energy value (ΔG_{ads}) is not possible because the molecular mass of the major component at the *Thymus algeriensis* essential oil components is not known. As the efficiency inhibition is essentially a function of the magnitude of its adsorption equilibrium constant K_{ads}, large values of K_{ads} are related to strong interaction between inhibitor molecules and the metal surface [47]. The inhibition process is due to the intermolecular synergistic effect between several constituents of the natural oil [47].

Table 4. Langmuir adsorption parameters.

Inhibitor	Slope	K_{ads} (L/g)	R^2
EOTA	1.16	13.95	0.99912

Effect of temperature

The effect of temperature on the inhibition efficiencies of EOTA was also studied by weight loss method in the temperature range 313-343 K. The values of corrosion rate in the absence and presence of optimum concentration of EOTA at different temperatures are given in Table 5. The fractional surface coverage θ can be easily determined from the weight loss measurements by the ratio η_{WL} (%) /100, where η_{WL} (%) is inhibition efficiency and calculated using relation 5. The data obtained suggest that EOTA get adsorbed on the mild steel surface at all temperatures studied and corrosion rates increased in absence and presence of inhibitor with increase in temperature in 1.0 M HCl solutions.

Table 5. Various corrosion parameters for mild steel in 1.0 M HCl in absence and presence of optimum concentration of essential oil at different temperatures

Temp (K)	Medium	C_R (mg/cm^2 h)	θ	η_{WL} (%)
313	Blank	1.230	—	—
	EOTA	0.012	0.980	98.0
323	Blank	1.920	—	—
	EOTA	0.042	0.978	97.8
333	Blank	3.890	—	—
	EOTA	0.094	0.975	97.5
343	Blank	6.260	—	—
	EOTA	0.196	0.960	96.0

The dependence of corrosion rate on temperature can be expressed by the Arrhenius equation [48]:

$$C_R = A\exp\left(-\frac{E_a}{RT}\right) \quad (8)$$

where C_R is the corrosion rate, E_a is the apparent activation energy of the mild steel dissolution, R is the molar gas constant, T is the absolute temperature, and A is the frequency factor. Arrhenius plots for the corrosion rate of mild steel are given in Fig. 8. Values of apparent activation energy of corrosion (E_a) were determined from the slope of Ln(C_R) vs. 1/T plots and shown in Table 6. The plots obtained are straight lines and the activation energy was evaluated from the slope of the straight line plots. The calculated values of activation energy are listed in Table 6. It can be seen in the table that E_a is higher in the presence of the inhibitor than in the absence of the inhibitor. This observation further supports the proposed physical adsorption mechanism.

Further insight into the adsorption mechanism is offered by considering the thermodynamic functions for the mild steel dissolution in 1.0 M HCl in the absence and presence of optimum concentration of EOAT (Fig. 9). In this regards, Transition state equation was used to evaluate the corrosion activation parameters, namely, the enthalpy of activation (ΔH_a) and entropy of activation (ΔS_a). Transition state equation is given by the expression [48]

$$C_R = \frac{RT}{Nh}\exp\left(\frac{\Delta S_a}{R}\right)\exp\left(-\frac{\Delta H_a}{RT}\right) \quad (9)$$

where h is Plank's constant, N is Avogrado's number, ΔS_a is the entropy of activation and ΔH_a is the enthalpy of activation.

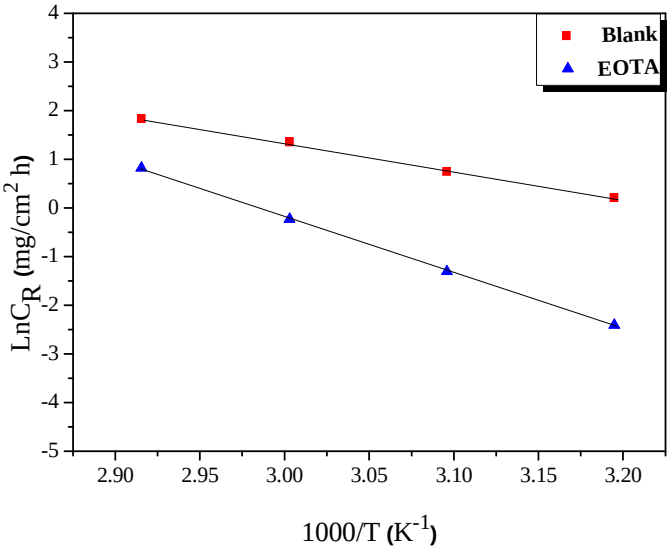

Figure 8: Arrhenius plots for mild steel corrosion rates (C_R) in 1.0 HCl in absence and in presence of 1.0 g/L of EOAT

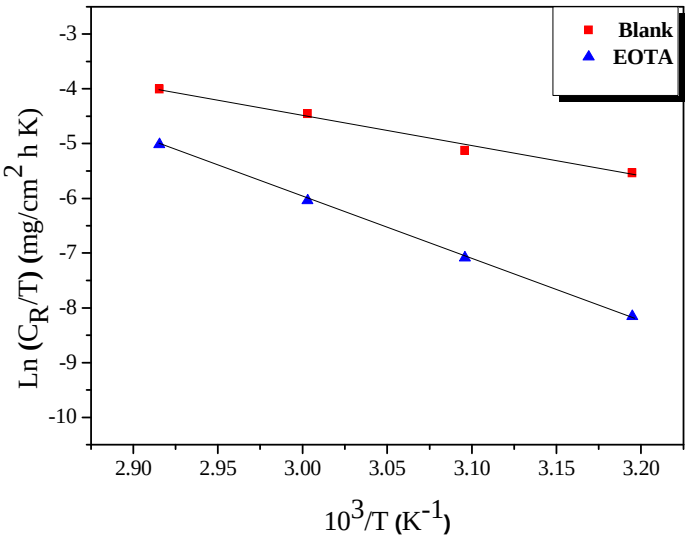

Figure 9: Transition-state plots for mild steel corrosion rates (C_R) in 1.0 M HCl in absence and in presence of 1.0 g/L of EOAT

The values of ΔH_a and ΔS_a are calculated and are given in Table 6. Inspection of these data revealed that the thermodynamic parameter (ΔH_a) for dissolution reaction of mild steel in 1.0 M HCl in the presence of extract is higher (93.39 KJ mol^{-1}) than that of in the absence of inhibitor (47.09 KJ mol^{-1}). The positive sign of ΔH_a reflect the endothermic nature of the steel dissolution process suggesting that the dissolution of mild steel is slow [49], in the presence of inhibitor. Large and negative value of entropie (ΔS_a) imply that the activated complex in the rate determining step represents an association rather than a dissociation step, meaning that a decrease in disordering takes place on going from reactant to the activated complex [50,51].

Table 6. Corrosion kinetic parameters for mild steel in 1.0 M HCl in absence and presence of 1.0 g/L of EOAT

Inhibitor	E_a (kJ mol^{-1})	ΔH_a (kJ mol^{-1})	ΔS_a (J mol^{-1} K^{-1})
Blank	49.06	47.09	-93.49
EOAT	96.02	93.39	-25.60

CONCLUSION

The studied *Thymus algeriensis* essential oil (EOTA) shows excellent inhibition properties for the corrosion of mild steel in 1.0 M HCl at 308 K, and the inhibition efficiency increases with increasing of the EOTA concentration. The inhibitor efficiencies determined by weight loss, Tafel polarisation and EIS methods are in reasonable agreement. Based on the polarisation results, the investigated junipers extract can be classified as mixed inhibitor. The calculated structural parameters show increase of the obtained R_{ct} values and decrease of the capacitance, C_{dl}, with EOTA concentration increase. It is suggested to attribute this to the increase of the thickness of the adsorption layer at steel surface. The adsorption model obeys to the Langmuir adsorption isotherm. The adsorption process is a spontaneous and exothermic process.

REFERENCES

[1] M. El Batouti, E. M. Elmelegy, A. A. Attia, A. M.Ahmed, *Mor. J. Chem.* 2**015**, 03, 484.
[2] M. Prajila, J. Sam, J. Bincy, J. Abraham, *J. Mater. Environ. Sci*. **2012**, 3, 1045.
[3] U.J. Naik, V.A. Panchal, A.S. Patel, N.K. Shah, *J. Mater. Environ. Sci.*, **2012**, 3, 935.
[4] A.H. Al Hamzi, H. Zarrok, A. Zarrouk, R. Salghi, B. Hammouti, S.S. Al-Deyab, M. Bouachrine, A. Amine, F. Guenoun, *Int. J. Electrochem*. Sci., **2013**, 8, 2586.
[5] A. Zarrouk**,** B. Hammouti, H. Zarrok, I. Warad, M. Bouachrine, *Der Pharm. Chem*., **2011**, 3, 263.
[6] D. Ben Hmamou, R. Salghi, A. Zarrouk, M. Messali, H. Zarrok, M. Errami, B. Hammouti, Lh. Bazzi , A. Chakir, *Der Pharm. Chem*., **2012**, 4, 1496.

[7] A. Ghazoui, N. Bencaht, S.S. Al-Deyab, A. Zarrouk, B. Hammouti, M. Ramdani, M. Guenbour, *Int. J. Electrochem. Sci*., **2013**, 8, 2272.
[8] A. Zarrouk, H. Zarrok, R. Salghi, N. Bouroumane, B. Hammouti, S.S. Al-Deyab, R. Touzani, *Int. J. Electrochem. S*ci., **2012**, 7, 10215.
[9] H. Bendaha, A. Zarrouk, A. Aouniti, B. Hammouti, S. El Kadiri, R. Salghi, R. Touzani, *Phys. Chem. N*ews, **2012**, 64, 95.
[10] S. Rekkab, H. Zarrok, R. Salghi, A. Zarrouk**,** Lh. Bazzi, B. Hammouti, Z. Kabouche, R. Touzani, M. Zougagh, *J. Mater. Environ. Sci*., **2012**, 3, 613.
[11] A. Zarrouk, B. Hammouti, H. Zarrok, M. Bouachrine, K.F. Khaled, S.S. Al-Deyab, *Int. J. Electrochem. Sci*., **2012**, 6, 89.
[12] A. Ghazoui, R. Saddik, N. Benchat, M. Guenbour, B. Hammouti, S.S. Al-Deyab, A. Zarrouk, *Int. J. Electrochem. Sci*., **2012**, 7, 7080.
[13] H. Zarrok, K. Al Mamari, A. Zarrouk, R. Salghi, B. Hammouti, S. S. Al-Deyab, E. M. Essassi, F. Bentiss, H. Oudda, *Int. J. Electrochem. Sci*., **2012**, 7, 10338.
[14] H. Zarrok, A. Zarrouk, R. Salghi, Y. Ramli, B. Hammouti, M. Assouag, E. M. Essassi, H. Oudda and M. Taleb, *J. Chem. Pharm. Res*., **2012**, 4, 5048.
[15] A. Zarrouk, B. Hammouti, A. Dafali, F. Bentiss, *Ind. Eng. Chem. Res.* **2013**, 52, 2560.
[16] H. Zarrok, A. Zarrouk, R. Salghi, H. Oudda, B. Hammouti, M. Assouag, M. Taleb, M. Ebn Touhami, M. Bouachrine, S. Boukhris, *J. Chem. Pharm. Res*. **2012**, 4, 5056.
[17] H. Zarrok, H. Oudda, A. El Midaoui, A. Zarrouk, B. Hammouti, M. Ebn Touhami, A. Attayibat, S. Radi, R. Touzani, *Res. Chem. Intermed*. **2012**, 38, 2051.
[18] A. Ghazoui, A. Zarrouk, N. Bencaht, R. Salghi, M. Assouag, M. El Hezzat, A. Guenbour, B. Hammouti, *J. Chem. Pharm. Res*. **2014**, 6, 704.
[19] H. Zarrok, A. Zarrouk, R. Salghi, M. Ebn Touhami, H. Oudda, B. Hammouti, R. Touir, F. Bentiss, S.S. Al-Deyab, *Int. J. Electrochem. Sci*. **2013**, 8, 6014.
[20] A. Zarrouk, H. Zarrok, R. Salghi, R. Touir, B. Hammouti, N. Benchat, L.L. Afrine, H. Hannache, M. El Hezzat, M. Bouachrine, *J. Chem. Pharm. Res*. **2013**, 5, 1482.
[21] H. Zarrok, A. Zarrouk, R. Salghi, M. Assouag, B. Hammouti, H. Oudda, S. Boukhris, S.S. Al Deyab, I. Warad, *Der Pharm. Lett*. **2013**, 5, 43.
[22] D. Ben Hmamou, M.R. Aouad, R. Salghi, A. Zarrouk, M. Assouag, O. Benali, M. Messali , H. Zarrok, B. Hammouti, *J. Chem. Pharm. Res*. **2012**, 4, 3498.
[23] M. Belayachi, H. Serrar, H. Zarrok, A. El Assyry, A. Zarrouk, H. Oudda, S. Boukhris, B. Hammouti, Eno E. Ebenso, A. Geunbour, *Int. J. Electrochem. Sci*. **2015**, 10, 3010.
[24] H. Tayebi, H. Bourazmi, B. Himmi, A. El Assyry, Y. Ramli, A. Zarrouk, A. Geunbour, B. Hammouti, Eno E.Ebenso, *Der Pharm. Lett*. **2014**, 6(6), 20.
[25] H. Tayebi, H. Bourazmi, B. Himmi, A. El Assyry, Y. Ramli, A. Zarrouk, A. Geunbour, B. Hammouti, *Der Pharm. Chem*. **2014**, 6(5), 220.
[26] P.R. Roberge, Corrosion inhibitors, Handbook of Corrosion Engineering, *McGraw-Hill*, New York, **1999**.
[27] S. Andreani, M. Znini, Paolini, L. Majidi, B. Hammouti, J. Costa, A. Muselli, *Int. J. Electrochem. Sci*. **2013**, 8, 11896.
[28] E. Stupnišek-Lisac, A. Gazivoda, M. Madžarac, *Electrochim. Acta* **2002**, 47, 4189.
[29] C.A. Loto, O. O. Joseph, R.T. Loto, A.P.I. Popoola, *Int. J. Electrochem. Sci*. **2013**, 8 11087.
[30] A.S. Mahdi, *Journal of Advanced Research in Engineering and Technology (IJARET)* **2014**, 5, 30.
[31] A.S. Mahdi, *Journal of Advanced Research in Engineering and Technology (IJARET)* **2014**, 5, 99.
[32] A. Singh, A. Kumar, T. Pramanik, *Orient. J. Chem.* **2013**, 29, 277.
[33] A. Bouyanzer, B. Hammouti, L. Majidi, *Mater. Letters* **2006**, 60, 2840.
[34] A. Bouyanzer, L. Majidi, B. Hammouti, *Bull. Elect.* **2006**, 22, 321.
[35] O. Ouachikh, A. Bouyanzer , M. Bouklah , J-M. Desjobert, J. Costa , B. Hammouti , L. Majidi *Surf. Rev. Lett.* **2009**, 16, 49.
[36] G. Cristofari, M. Znini, L. Majidi, A. Bouyanzer, S. Al-Deyab, J. Paolini, B. Hammouti, J. Costa, *Int. J. Electrochem. Sci*. **2011**, 6, 6699.
[37] M. Benabdellah, M. Bendahou, B. Hammouti, M. Benkaddour, *Appl. Surf. Sci*. **2005**, 252, 6212.
[38] ASTM, G 31-72, American Society for Testing and Materials, Philadelphia, PA, **1990**.
[39] I. Ahamad, R. Prasad, M.A. Quraishi, *Corros. Sci*. **2010**, 52, 933.
[40] F. Bentiss, M. Outirite, M. Traisnel, H. Vezin, M. Lagrenée, B. Hammouti, S.S. Al-Deyab, C. Jama, *Int. J. Electrochem. Sci*. **2012**, 7, 1699.
[41] O.L. Riggs, Jr Corrosion inhibitors, 2nd edn. C.C. Nathan, Houston, TX, **1973**.
[42] A.K. Singh, M.A. Quraishi, *Corros. Sci*. **2010**, 52, 1529.
[43] K.F. Khaled, N. Hackerman, *Electrochim Acta* **2003**, 48, 2715.
[44] R. Rosliza, W.B. Wan Nik, H.B. Senin, *Mater. Chem. Phys*. **2008**, 107, 281.

[45] F.M. Reisde, H.G. Melo, I. Costa, *Electrochim. Acta* **2006**, 51, 1780.
[46] M. Abdel-Gaber, B.A. Abd-El-Nabey, I.M. Sidahmed, A.M. El-Zayaday, M. Saadawy, *Corros. Sci*. **2006**, 48, 2765.
[47] K. M. Emran, N. M. Ahmed, B. A. Torjoman, A. A. Al-Ahmadi , S. N. Sheekh, *J. Mater. Environ. Sci.* **2014**, 5, 1940.
[48] J.O'M. Bockris, A.K.N. Reddy, Modern Electrochemistry, *Plenum Press*, New York, **1977**, 2, 1267.
[49] N.M. Guan, L. Xueming, L. Fei, *Mater. Chem. Phys*. **2004**, 86, 59.
[50] N. Soltani, M. Behpour, S.M. Ghoreishi, H. Naeimi, *Corros. Sci*. **2010**, 52, 1351.
[51] M.K. Gomma, M.H. Wahdan, *Mater. Chem. Phys*. **1995**, 39, 209.